

Geometry-Biased Transformer for Robust Multi-View 3D Human Pose Reconstruction

Olivier Moliner^{1,2}, Sangxia Huang² and Kalle Åström¹

¹ Centre for Mathematical Sciences, Lund University, Sweden

² Sony Corporation, Lund Laboratory, Sweden

Abstract— We address the challenges in estimating 3D human poses from multiple views under occlusion and with limited overlapping views. We approach multi-view, single-person 3D human pose reconstruction as a regression problem and propose a novel encoder-decoder Transformer architecture to estimate 3D poses from multi-view 2D pose sequences. The encoder refines 2D skeleton joints detected across different views and times, fusing multi-view and temporal information through global self-attention. We enhance the encoder by incorporating a geometry-biased attention mechanism, effectively leveraging geometric relationships between views. Additionally, we use detection scores provided by the 2D pose detector to further guide the encoder’s attention based on the reliability of the 2D detections. The decoder subsequently regresses the 3D pose sequence from these refined tokens, using pre-defined queries for each joint. To enhance the generalization of our method to unseen scenes and improve resilience to missing joints, we implement strategies including scene centering, synthetic views, and token dropout. We conduct extensive experiments on three benchmark public datasets, Human3.6M, CMU Panoptic and Occlusion-Persons. Our results demonstrate the efficacy of our approach, particularly in occluded scenes and when few views are available, which are traditionally challenging scenarios for triangulation-based methods.

I. INTRODUCTION

3D human pose estimation is a fundamental problem in computer vision with applications in many domains, including sports analysis, robotics, virtual reality, and character animation. Accurate 3D pose estimation is essential for many of these applications, as it enables understanding human motion, behaviour, and interaction with the environment.

Although 3D pose estimation methods from monocular images or videos have achieved impressive progress in recent years [21], [23], [36], [25], [30], estimating human pose in 3D from a single viewpoint is a challenging task, vulnerable to occlusion and inherently ill-posed due to depth ambiguities.

A natural alternative to overcome these limitations is to estimate 3D human poses from multiple camera viewpoints, which enables reconstruction without depth ambiguity and, given calibrated cameras, in absolute world coordinates. Multi-view 3D pose estimation methods usually operate in two steps: estimating 2D poses in each view, then reconstructing the 3D poses from the 2D poses using for example triangulation [7]. As the reconstruction quality depends greatly on the quality of the 2D poses, many works focus

on improving these by fusing 2D features across views [10], [42], [8], [29], [17], [38].

Most public multi-view human pose datasets are characterized by a central capture area, overlapping views and no occlusions. In real applications, however, multi-view camera systems are subject to constraints such as cost, room layout, the presence of furniture or the availability of electrical outlets, resulting in wide-baseline setups with few cameras, strong occlusions, areas where few views overlap and subjects moving in and out of view. These are settings in which triangulation-based methods typically struggle. Moreover, large rooms or outdoor scenes may require wireless distributed systems in which it is not practical to transmit images or intermediate 2D feature maps for real-time applications.

To address these issues, we approach multi-view, single-person 3D human pose reconstruction as a regression problem and propose a novel encoder-decoder Transformer architecture to estimate 3D poses from multi-view 2D skeleton sequences. We treat all 2D joints detected in different views at different times as individual tokens and feed them to the encoder, which fuses multi-view and temporal information using global self-attention. We propose a geometry-biased attention mechanism to leverage the geometric relationships between different views. Additionally, we use the detection scores provided by the 2D pose detector to further guide the encoder’s attention based on the reliability of the 2D detections. Finally, we regress the 3D poses by querying this set-latent representation of the multi-view pose sequence with a Transformer decoder, using a pre-defined query for each joint.

Our main contributions are summarized as follows:

- We present a new transformer-based method for multi-view, single-person 3D human pose reconstruction, which effectively fuses multi-view and temporal information.
- We introduce confidence and geometry biases to guide the encoder’s attention mechanism using the known structure of the problem.
- We propose scene centering, synthetic views and token dropout to promote generalization to unseen scenes and make our model resilient to missing joints.
- We analyze the performance of our method through ablation studies and show that it outperforms state-of-the-art methods in occluded scenes and when few overlapping views are available.

This work was partially supported by the Wallenberg AI, Autonomous Systems and Software Program (WASP) funded by the Knut and Alice Wallenberg Foundation.

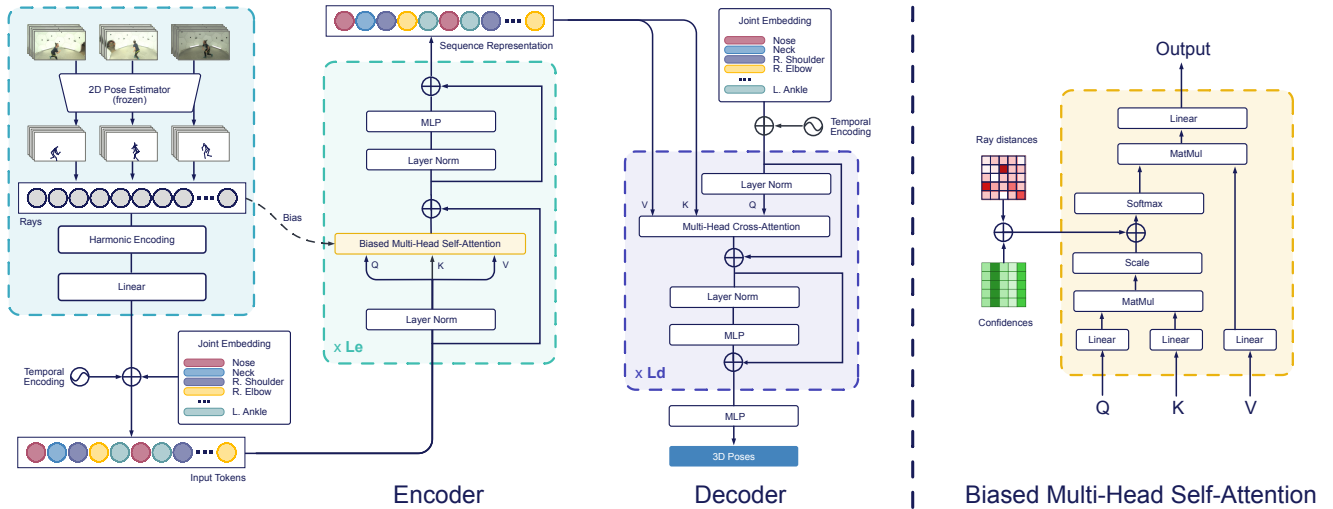


Fig. 1. **Overview of our proposed method.** We obtain 2D pose sequences from multiple views and encode them into a set of joint tokens. The tokens are processed by a Transformer encoder, yielding a sequence representation via self-attention. The encoder is biased with detection confidence scores and pairwise ray distances (right). We decode the sequence representation in a Transformer decoder by cross-attention with a set of predefined joint queries. Finally we regress the 3D coordinates of the joints with an MLP.

The remainder of this paper is organized as follows: Section II discusses previous works related to 3D human pose estimation. Section III presents the details of our proposed method, including the encoder-decoder Transformer architecture with biased self-attention. Section IV reports the experimental results and comparisons with existing methods. Finally, Section V concludes the paper and discusses possible future directions.

II. RELATED WORK

3D Human Pose Estimation. Many 3D human pose estimation works focus on monocular images or videos [21], [23], [36], [25], [30]. This is however an ill-posed problem due to depth ambiguities and occlusions. A natural solution to overcome this issue is to estimate 3D poses from multiple views, which is not prone to depth ambiguities. Moreover, a body part that is occluded in one view may become visible in other views. Multi-view 3D pose estimation is usually performed in two steps: first extracting 2D keypoints from each view independently with a 2D pose detector, then reconstructing the 3D poses via triangulation [10], [42], [8], [29], [17], [38] or pictorial structure models [2], [24], [27]. As the accuracy of the reconstruction step greatly depends on the quality of the keypoints obtained at the first step, several recent methods focus on refining the 2D pose detections by fusing information between views. Qiu *et al.* [27] proposed to learn a fixed attention matrix to retrieve 3D poses from 2D views. However, the fusion network needs to be re-trained if the camera configuration changes. Isakov *et al.* [10] train a 2D detector while solving a multi-view 3D reconstruction problem via differentiable triangulation. They also propose to learn 3D pose directly by fusing features in 3D voxel feature maps. While very accurate, volumetric approaches are computationally expensive. Several methods focus on refining the detector’s intermediate feature maps by

leveraging epipolar geometry [42], [8] or a relaxation thereof [17]. In particular, AdaFuse [42] tackles the occlusion issue by learning an adaptive fusion weight to reduce the impact of low-quality views. However, it discards information off the epipolar line and treats each joint independently.

Transformers for 3D Pose Estimation The Transformer [34] has proven to be a powerful architecture with broad applications in various fields, from natural language processing [34], [5] to computer vision [4], [3]. Several researchers have applied Transformers to 2D human pose estimation [20], [37], [39]. Metro [15] uses a Transformer to directly regress 3D poses and meshes from monocular images. MixSTE [40] performs 3D pose estimation from videos by alternating spatial and temporal attention.

Recently, researchers have used Transformers for multi-view 3D pose estimation. He *et al.* proposed the Epipolar Transformer [8], which refines the intermediate features of a 2D detector for a reference view by using features of corresponding points along the epipolar line in neighbouring views. TransFusion [17] performs cross-view fusion via global attention. They introduce the epipolar field to encourage high similarity between pixels located close to each other’s epipolar line. Global attention between 2D feature maps is however computationally expensive. To alleviate this cost, Ma *et al.* proposed to prune visual tokens based on the attention scores of keypoint queries [18]. In this study, we present an encoder-decoder transformer model operating on 2D joint coordinates and associated confidence scores, which is a much sparser input.

III. METHOD

A. Overview

Figure 1 provides an overview of our proposed multi-view 3D human pose reconstruction method. We use an off-the

shelf 2D human pose detector [33] to extract 2D skeletons from a sequence of multi-view images capturing the scene from different viewpoints. We flatten these poses to a set of joints, and transform them into 3D rays traced through each 2D joint detection and the corresponding camera center. We project the rays independently to high-dimensional features and refine this set of feature vectors via self-attention in a Transformer encoder, yielding a global set-latent representation for the whole sequence. We use prior knowledge about geometry and detection scores to guide the attention layers of the encoder. Finally, we predict the 3D poses with a Transformer decoder by querying the sequence encoding with a set of target feature vectors describing the semantics of the points to decode.

B. Ray Encoding

Our model takes as input a multi-view sequence of 2D poses with associated confidence scores $\mathbf{S} \in \mathbb{R}^{T_{in} \times C \times J \times 3}$, along with extrinsic camera matrices $\{\mathbf{E}_c = [\mathbf{R}_c | \mathbf{t}_c] \in SE(3)\}_{c=1}^C$ and intrinsic parameters $\{\mathbf{K}_c \in \mathbb{R}^{3 \times 3}\}_{c=1}^C$, where C is the number of cameras, T_{in} is the number of time frames and J is the number of keypoints of the detected poses.

We flatten the sequence to a set of individual joints, which we transform using the camera matrices into 3D rays passing through the estimated 2D joints and the corresponding camera centers. With perfect camera calibration and perfect detections, these rays would also pass through the corresponding 3D joints. We use the Plücker representation for the rays [26], [12], [32], [35], as it decouples the ray coordinates from the positions of the camera centers along the rays, thus promoting generalization to novel camera configurations. Specifically, for a joint j with pixel coordinates (u, v) in camera c , we calculate the Plücker coordinates $\mathbf{r}_{j,c} \in \mathbb{R}^6$ of the ray as

$$\mathbf{r}_{j,c} = (\mathbf{d}_{j,c}, \mathbf{m}_{j,c}) = (\tilde{\mathbf{d}}_{j,c}, \mathbf{t}_c \times \tilde{\mathbf{d}}_{j,c}) / \|\tilde{\mathbf{d}}_{j,c}\|, \quad (1)$$

where $\tilde{\mathbf{d}}_{j,c}$ is the ray direction:

$$\tilde{\mathbf{d}}_{j,c} = \mathbf{R}_c^{-1} \mathbf{K}_c^{-1} \begin{pmatrix} u \\ v \\ 1 \end{pmatrix}. \quad (2)$$

Finally, we form the ray embeddings as follows:

$$\mathbf{f}_{j,c} = \mathbf{W}_r(h(\mathbf{r}_{j,c})), \quad (3)$$

where $h(\cdot)$ denotes harmonic embedding [22] and \mathbf{W}_r is a linear projection layer.

C. Biased Transformer Encoder

We process the ray embeddings using a Transformer encoder [34] consisting of L_e layers of global multi-head self-attention. This allows to model relationships between body joints, across views and along the time dimension simultaneously, providing global context to each token. As the Transformer is permutation-invariant, we add to the tokens a learned body joint embedding and a harmonic temporal encoding based on the relative timestamps of the observations from the current time step, thus retaining temporal and body structure information.

At the core of the Transformer architecture, the attention mechanism computes a weighted sum of a set of tokens based on their relevance to a particular query. In particular, scaled dot-product attention calculates the relevance score of each key \mathbf{K} with respect to a query \mathbf{Q} :

$$\text{Attention}(\mathbf{Q}, \mathbf{K}, \mathbf{V}) = \text{softmax}\left(\frac{\mathbf{Q}\mathbf{K}^T}{\sqrt{d_k}}\right) \mathbf{V}, \quad (4)$$

where \mathbf{Q}, \mathbf{K} , and \mathbf{V} are projections of the input tokens and d_k is the dimension of the feature vectors.

Our problem has known structure, which we can use to guide the transformer during self-attention. First, the pose detector provides confidence scores indicating the reliability of the predicted coordinates. Intuitively, when calculating the attention matrix more weight should be given to tokens corresponding to joints with high confidence scores. To incorporate this knowledge about joint confidence, we bias the attention matrix by adding the confidence matrix \mathbf{M}_{conf} , obtained by repeating the row-vector of the keys' detection confidence scores q times row-wise. For each query, this will increase the attention score of keys corresponding to joints with high confidence scores.

We also posit that a token should attend more to tokens corresponding to the same body joint seen from different cameras and to tokens corresponding to other joints of the body seen from the same viewpoint. These correspond to rays that are closer in 3D space. Similarly to [35], we form the matrix \mathbf{M}_{dist} of pairwise distances between the rays, and use it as a geometry bias to the attention map. Given two rays $\mathbf{r}_q = (\mathbf{d}_q, \mathbf{m}_q), \mathbf{r}_k = (\mathbf{d}_k, \mathbf{m}_k)$ with *unit* directions \mathbf{d}_q and \mathbf{d}_k , their distance is given by

$$d(\mathbf{r}_q, \mathbf{r}_k) = \begin{cases} \frac{|\mathbf{d}_q \cdot \mathbf{m}_k + \mathbf{d}_k \cdot \mathbf{m}_q|}{\|\mathbf{d}_q \times \mathbf{d}_k\|}, & \mathbf{d}_q \times \mathbf{d}_k \neq 0 \\ \|\mathbf{d}_q \times (\mathbf{m}_q - \mathbf{m}_k)\|, & \text{otherwise.} \end{cases} \quad (5)$$

We multiply the distance matrix by a negative factor, learned independently for each encoder layer. Hence rays with large distance to query rays will be penalized, while intersecting rays, such as rays from the same camera, will have a pairwise distance of 0 and will not be penalized. Rays corresponding to different views of the same joint at the same time will typically have small pairwise distances, but outliers will be further away from other observations of the same joint and will incur a penalty. This relates the geometry bias to epipolar geometry, as the attention score will be higher for joint detections along the epipolar line of the query joint.

At each layer l of the encoder, we thus calculate the following biased attention map:

$$\mathbf{A}_l = \text{softmax}\left(\frac{\mathbf{Q}\mathbf{K}^T}{\sqrt{d_k}} + \eta_l^2 \mathbf{M}_{conf} - \gamma_l^2 \mathbf{M}_{dist}\right), \quad (6)$$

where η_l and γ_l are learnable parameters for each layer.

D. 3D pose sequence decoding

The output of the encoder is a set of feature vectors representing the whole pose sequence. To extract information about specific joints at given times, we construct a predefined

query providing the semantics of the points to decode. It consists in J learned embedding vectors corresponding to each human keypoint, repeated T_{out} times, where T_{out} is the desired time range. We add harmonic temporal encoding to specify the timing of each point. We decode the 3D pose sequence using a Transformer decoder, which attends to the set of feature vectors with several layers of multi-head cross-attention with the predefined query. Finally, we regress the 3D world coordinates of the joints from the decoded tokens using a Multi-Layer Perceptron (MLP).

The query does not need to comprise the same number of frames as the input¹. Moreover, the number of input and output frames can be chosen to be different during training and inference.

E. Training and Inference

The model is trained by minimizing the Mean Squared Error (MSE)

$$\mathcal{L} = \frac{1}{NT_{out}J} \sum_{i=1}^N \sum_{t=1}^{T_{out}} \sum_{j=1}^J \|P_{itj} - \hat{P}_{itj}\|^2, \quad (7)$$

where N is the number of poses in the dataset, P_{itj} is a ground-truth 3D joint and \hat{P}_{itj} is the corresponding prediction.

We train our model to reconstruct the whole sequence of length $T_{out} = T_{in}$. During inference, we input T_{in} frames of observations, i.e. the latest observation and $T_{in} - 1$ past observations, but we are only interested in reconstructing the latest frame, i.e. $T_{out} = 1$, regardless of T_{in} . Hence our model can make fully causal predictions and is well-suited for real-time inference.

F. Promoting Generalization

Multi-view pose datasets with 3D annotations are relatively small, and are usually collected in controlled environments with fixed capture area, few camera poses and no occlusions. To enable our model to handle unseen scenes and camera configurations, we introduce the following methods during training and inference.

Centering. To enable the model to generalize to scenes of arbitrary dimensions, we *roughly* center the scene around the subject during training and inference. During training, given an input sequence of length T_{in} , we select a random ground-truth pose at time t and project its neck joint on the floor. We add random noise on the plane to this projection, and transform all observation rays and ground-truth poses of the sequence to a coordinate system centered on the resulting point. Finally, we rotate the scene around the vertical axis with a random angle. During inference, at the first time step the 3D rays can be centered around a point obtained by triangulation of the observations, without rotating the scene. At subsequent time steps, the coordinate system is centered around the predicted 3D pose obtained at the previous time step.

¹In fact, the query does not even need to contain the same number of joints as the input, although this is not something we explore here.

As shown in Sec. IV-G, transforming the scene to this body-centric coordinate system allows our model to better generalize to scenes with unseen dimensions.

Synthetic views. Existing multi-view datasets with ground-truth 3D pose annotations have fixed, limited camera pose configurations. This can limit the generalization capabilities of learning-based pose reconstruction methods. One way to mitigate this issue is through the use of synthetic data. During training, we generate synthetic 2D poses in addition to the observations provided by the datasets. Specifically, we sample random camera positions and calculate the rays passing through these and each joint of the ground-truth 3D poses.

Token dropout. To make our model resilient to missing data, we randomly remove 20% of the input tokens during training, employing a similar technique as [16]. As a consequence, a given joint may be invisible in all views during the whole sequence, or the whole body may be missing at given times. This further encourages the model to aggregate information from the whole body and across time frames. Token dropout has the convenient side-effect of reducing computing and memory requirements during training.

IV. EXPERIMENTS

We evaluate our method on three large-scale multi-view datasets for multi-view 3D human pose estimation: Human3.6M [9], CMU Panoptic [13] and Occlusion-Person [42]. We inspect our method’s ability to handle occlusions and scenes with few views, and test its ability to generalize to new datasets. We also compare our results to the state of the art and conduct ablation studies to validate the effectiveness of the components of our method.

A. Datasets and Evaluation Metrics

Human 3.6M [9] consists of 3.6 million images of 11 subjects performing various activities in an indoor environment, with corresponding 3D poses. The images are captured at 50 Hz by 4 synchronized cameras placed approximately at the corners of a $4\text{m} \times 10\text{m}$ rectangle. The ground truth 3D pose annotations are obtained by a marker-based motion capture system. We follow standard practice and use 5 subjects for training (S1, S5, S6, S7, S8) and 2 subjects for testing (S9, S11). Some sequences with the ‘S9’ validation subject have erroneous 3D annotations and were ignored during evaluation as in [10]: parts of ‘Greeting’, ‘SittingDown’ and ‘Waiting’. To test the performance of our method under occlusion, we adopt the method of [31], [41] to create a test dataset derived from H36M, *H36M-Occl*, in which we simulate occlusion scenarios by randomly placing white square masks over the 2D joint, with a probability of 0.1.

CMU Panoptic [13] contains multiple scenes in which people perform different activities in an indoor environment. Images are captured by hundreds of VGA cameras and 31 HD cameras installed on a hemispherical structure of diameter 5.5m. The 3D pose annotations are obtained by triangulation using all camera views. We use the same train/test sequences as Isakov *et al.* [10], consisting of

TABLE I

RECONSTRUCTION ERROR ON H36M DATASET WITH FEWER CAMERAS. ABSOLUTE MPJPE (MM). "†": POSE DETECTOR FINE-TUNED ON H36M.

Method		Number of Cameras		
		2	3	4
Alg. Tri. [10]	(ResNet-152)†	51.1	23.4	19.1
Ours	(ResNet-152)†	29.9	24.4	22.7
Alg. Tri.	(HRNet)	120.7	50.9	44.2
Ours	(HRNet)	36.8	30.4	26.0

TABLE III

RECONSTRUCTION ERROR ON OCCLUSION-PERSON. ABSOLUTE MPJPE (MM). "†": POSE DETECTOR FINE-TUNED ON THE DATASET.

Method	Number of Cameras			
	2	3	4	8
RANSAC† [42]	33.7	87.5	35.0	15.5
ScoreFuse† [42]	32.7	25.7	21.4	15.0
AdaFuse† [42]	-	26.2	19.7	12.6
Ours (HRNet)	30.8	22.9	19.6	14.2

scenes featuring a single person. Unless otherwise stated, we use 4 HD cameras (2,13,10,19) for testing and the remaining 27 HD cameras for training.

Occlusion-Person [42] is a synthetic dataset rendered with UnrealCV [28] in which thirteen human models driven by motion sequences from the CMU Motion Capture database [1] are put into nine scenes featuring occluding objects and captured by 8 cameras. We use the same train/test sequences as Zhang *et al.* [42].

Evaluation metric. We evaluate the 3D pose reconstruction accuracy using the absolute Mean Per Joint Position Error (MPJPE), which is the average of the L2 distance between the prediction and the ground truth for each joint, measured in millimeters. We do not align the estimated 3D poses and ground truth in any way.

B. Implementation Details

We undistort the images using the camera parameters provided with the datasets and extract the 2D poses with a pre-trained pose detector which remains frozen when training our network. Unless otherwise indicated, we use HRNet-W32 [33], trained on COCO, with YoloX [6] box proposals. For the harmonic embedding h , we use 15 frequencies. We use 3 layers for the transformer encoder and 2 layers for the decoder. Both encoder and decoder have 6 heads. During training, we input 9 time frames and 2 randomly sampled views, and also output 9 frames. Unless otherwise stated, during evaluation we input 9 time frames and only output 1 frame, corresponding to the latest observation.

We train our model with the Adam optimizer [14] for 300000 iterations with a mini-batch size of 256. The initial learning rate is 10^{-4} . It is smoothly decayed after a warmup

TABLE II

RECONSTRUCTION ERROR ON THE H36M-OCCL TEST DATASET. ABSOLUTE MPJPE (MM). "†": POSE DETECTOR FINE-TUNED ON H36M.

Method		Number of Cameras		
		2	3	4
Alg. Tri. [10]	(ResNet-152)†	163.3	39.5	27.9
Ours	(ResNet-152)†	39.1	33.4	31.3
Alg. Tri.	(HRNet)	217.3	72.4	54.1
Ours	(HRNet)	42.3	34.5	31.6

phase of 10 k steps. Training takes about 5 hours on a single Nvidia RTX 4090.

C. Impact of Varying Number of Views

We measure the performance of our method on the H36M dataset when fewer camera views are available. To compare with the Algebraic Triangulation method in [10], we train and test our network on 2D poses provided by the ResNet-152 detector from Iskakov *et al.* We also compare our method to the Algebraic Triangulation method applied to HRNet poses. We test all methods with different numbers of input views, and present the average error obtained with all combinations of views. The results are shown in Tab. I. With the high-quality ResNet-152 poses, Algebraic Triangulation yields superior results with 3 and 4 views, but the reconstruction accuracy drops considerably when only 2 views are available, possibly due to self-occlusions. On the other hand, our method’s accuracy does not drop as much when using only 2 views. When using poses extracted with the off-the shelf detector, our method consistently achieves lower reconstruction error regardless of the number of views.

D. Occlusion handling

We evaluate our method’s ability to handle occlusions on the H36M-Occl test dataset, using the model trained on the original H36M training set without occlusions. As shown in Tab. II, when using the ResNet-152 detector, fine-tuned on H36M, triangulation yields the best results when enough cameras are available. However, with fewer than four cameras our method provides significantly better results. Also, when using the off-the-shelf HRNet pose detector, our method yields superior results compared to the baseline with any number of cameras.

We also compare our method to Adafuse [42] and its baselines on the Occlusion-Person dataset. For all methods in [42], 3D joints are reconstructed independently, using triangulation, hence we only calculate the error for joints visible in at least 2 views. For our method, on the other hand, we present the error for all joints, including joints that are not visible in any view. As shown in Tab. III, our method achieves competitive results when all camera views are used. In this setting, however, most joints are visible in at least 4 views. Therefore, we also compare the methods with different numbers N_c of input views, and present the average error obtained with all combinations of N_c cameras.

TABLE IV

GENERALIZATION BETWEEN DATASETS. WE TRAIN OUR MODEL ON THE CMU PANOPTIC DATASET AND TEST ON H36M. ABSOLUTE MPJPE (MM).

Method	Dir	Disc	Eat	Greet	Phone	Pose	Purch	Sit	SitD	Smoke	Photo	Wait	Walk	WalkD	WalkT	Avg
Alg. Tri. (HRNet)	44.6	43.5	42.2	42.5	43.7	41.6	48.5	46.8	51.7	45.4	45.7	42.3	40.3	45.6	39.8	44.3
Ours (HRNet)	33.9	32.5	32.6	33.7	38.3	30.8	35.1	56.9	85.9	36.0	37.9	33.3	29.1	38.7	28.7	38.9

TABLE V

COMPARISON WITH STATE-OF-THE-ART METHODS. ABSOLUTE MPJPE (MM) ON THE HUMAN3.6M DATASET. "†": 2D POSE DETECTOR FINE-TUNED ON THE TARGET DATASET.

Method	H36M	CMU
Cross View Fusion [27]†	26.2	-
RANSAC Baseline [10]	-	33.4
Algebraic Triangulation [10]†	19.2	21.3
Volumetric [10]†	17.7	13.7
Remelli et al. [29]†	30.2	-
Epipolar Transformers [8]†	27.1	-
TransFusion [17]†	25.8	-
Ours (ResNet-152)†	22.7	-
Algebraic Triangulation (HRNet)	44.2	26.2
Ours (HRNet)	26.0	17.2

When the number of available views decreases, our method yields the smallest reconstruction errors, further highlighting its ability to handle occluded scenes.

E. Generalization Between Datasets

To examine if our proposed approach generalizes between datasets, we train our model on the CMU Panoptic dataset and test it on H36M. Following [10], we calculate the error on joints that have similar 3D annotations in both datasets (shoulder, elbow, wrist, knee, ankle). As can be seen in Tab. IV, our method yields a lower error than the baseline, demonstrating the ability of our model to generalize to unseen camera settings and positions. However, the results also show that our model struggles to reconstruct correct poses for the sitting sequences. These sequences contain body poses that are not present in the CMU Panoptic dataset, which highlights a limitation of our method.

F. Comparison with other methods

In Tab. V, we compare our method with previous work on the H36M and CMU Panoptic datasets. Other methods use 2D pose detectors fine-tuned on the target dataset. To provide a fair comparison, we train our model on 2D poses obtained with the detector from [10]. In this setting, it achieves competitive results. To consider a more realistic scenario, we use off-the-shelf algorithms to detect human bounding boxes and extract 2D poses. As we are not aware of other methods providing absolute pose reconstruction results for off-the-shelf detectors, we apply the Algebraic Triangulation method from [10] to the HRNet detections and compare to our method. Here, our approach achieves superior results compared to the baseline.

TABLE VI

ABLATION STUDY ON THE COMPONENTS OF OUR FRAMEWORK. WE REMOVE EACH FEATURE IN TURN AND TRAIN ON THE CMU PANOPTIC AND H36M DATASETS. WE REPORT THE 3D POSE ESTIMATION ERROR MPJPE (MM).

	Centering	Synthetic	Confidence bias	Geometry bias
	-	✓	✓	✓
	-	-	✓	✓
	-	-	-	✓
	-	-	-	-
	✓	✓	✓	✓

Train	Test	CMU	H36M	H36M-Occl
CMU	CMU	22.4	18.9	19.3
H36M	H36M	39.0	49.2	40.6
H36M	H36M-Occl	43.1	52.3	44.0
CMU	H36M	101.2	57.2	55.7

TABLE VII

EFFECT OF THE NUMBER OF TIME FRAMES. ABSOLUTE MPJPE (MM). WE EVALUATE THE SAME MODEL TRAINED ON H36M WITH HRNET DETECTIONS, USING 4 CAMERA VIEWS.

Dataset	Number of Time Frames				
	1	2	3	6	9
H36M	29.4	27.9	27.7	27.3	26.0
H36M-Occl	41.5	34.9	34.0	32.5	31.6

G. Ablation Studies

We evaluate the usefulness of the components of our method by removing them in turn. For each ablation, we present results with various combinations of training and test datasets. As seen in Tab. VI, the reconstruction accuracy degrades when the geometry and confidence biases are removed. When conducting intra-dataset evaluations, the advantages of synthetic views and centering are unclear; however, they significantly enhance accuracy when generalizing between datasets. This is likely due to the significant difference in size between the capture areas of the H36M and CMU datasets.

We also study the effect of the number of input time frames. We report the results of our method on H36M and H36M-Occl, using 4 views and HRNet 2D detections as input. We use the same model trained on H36M. As shown in Tab. VII, increasing the input sequence length improves reconstruction accuracy. Temporal information is particularly significant under occlusion. Even providing only one previous time frame of observations has a strong effect.

V. CONCLUSION

We presented a novel approach for 3D human pose reconstruction using 2D pose data from multiple viewpoints, leveraging a Transformer-based encoder-decoder architecture with biased self-attention. It can straightforwardly accommodate any 2D pose detection network and is suitable for wide-baseline, real-time systems. Experiments on three large-scale datasets show that our method consistently outperforms triangulation-based methods under heavy occlusion and when fewer input views are available. One of the major limitations of our approach is its difficulty in reconstructing unseen human poses. One potential strategy to mitigate this challenge is to pre-train the network on large-scale 3D motion capture datasets such as [19]. There may also be a benefit in exploring self-supervised training, which would enable our network to be trained on substantially larger datasets without 3D annotations. Further interesting avenues for future work include improving the model's performance by decoupling the size of the latent set from the number of the inputs in a way similar to [11], and extending our approach to accommodate multi-person settings.

REFERENCES

- [1] Carnegie Mellon University Graphics Lab Motion Capture Database. <http://mocap.cs.cmu.edu>, 2003.
- [2] M. Burenius, J. Sullivan, and S. Carlsson. 3d pictorial structures for multiple view articulated pose estimation. In *Proceedings of the IEEE Conference on Computer Vision and Pattern Recognition (CVPR)*, June 2013.
- [3] N. Carion, F. Massa, G. Synnaeve, N. Usunier, A. Kirillov, and S. Zagoruyko. End-to-End object detection with transformers. In A. Vedaldi, H. Bischof, T. Brox, and J.-M. Frahm, editors, *Computer Vision – ECCV 2020*, pages 213–229, Cham, 2020. Springer International Publishing.
- [4] A. Dosovitskiy, L. Beyer, A. Kolesnikov, D. Weissenborn, X. Zhai, T. Unterthiner, M. Dehghani, M. Minderer, G. Heigold, S. Gelly, J. Uszkoreit, and N. Houlsby. An image is worth 16x16 words: Transformers for image recognition at scale. *ICLR*, 2021.
- [5] S. Edunov, M. Ott, M. Auli, and D. Grangier. Understanding back-translation at scale. In *Proceedings of the 2018 Conference on Empirical Methods in Natural Language Processing*, pages 489–500, Brussels, Belgium, Oct.-Nov. 2018. Association for Computational Linguistics.
- [6] Z. Ge, S. Liu, F. Wang, Z. Li, and J. Sun. YOLOX: Exceeding YOLO series in 2021. July 2021.
- [7] R. Hartley and A. Zisserman. *Multiple View Geometry in Computer Vision*. Cambridge University Press, New York, NY, USA, 2 edition, 2003.
- [8] Y. He, R. Yan, K. Fragkiadaki, and S.-I. Yu. Epipolar transformers. In *Proceedings of the IEEE/CVF conference on computer vision and pattern recognition*, pages 7779–7788, 2020.
- [9] C. Ionescu, D. Papava, V. Olaru, and C. Sminchisescu. Human3.6M: Large scale datasets and predictive methods for 3D human sensing in natural environments. *IEEE Trans. Pattern Anal. Mach. Intell.*, 36(7):1325–1339, July 2014.
- [10] K. Isakov, E. Burkov, V. Lempitsky, and Y. Malkov. Learnable triangulation of human pose. In *International Conference on Computer Vision (ICCV)*, 2019.
- [11] A. Jaegle, S. Borgeaud, J.-B. Alayrac, C. Doersch, C. Ionescu, D. Ding, S. Koppula, D. Zoran, A. Brock, E. Shelhamer, O. J. Henaff, M. Botvinick, A. Zisserman, O. Vinyals, and J. Carreira. Perceiver IO: A general architecture for structured inputs & outputs. In *International Conference on Learning Representations*, 2022.
- [12] Y.-B. Jia. Plücker coordinates for lines in the space. *Problem Solver Techniques for Applied Computer Science, Com-S-477/577 Course Handout*, 3, 2020.
- [13] H. Joo, T. Simon, X. Li, H. Liu, L. Tan, L. Gui, S. Banerjee, T. Godisart, B. Nabbe, I. Matthews, T. Kanade, S. Nobuhara, and Y. Sheikh. Panoptic studio: A massively multiview system for social interaction capture. *IEEE transactions on*, Dec. 2016.
- [14] D. P. Kingma and J. Ba. Adam: A method for stochastic optimization. In Y. Bengio and Y. LeCun, editors, *3rd International Conference on Learning Representations, ICLR 2015, San Diego, CA, USA, May 7-9, 2015, Conference Track Proceedings*, 2015.
- [15] K. Lin, L. Wang, and Z. Liu. End-to-end human pose and mesh reconstruction with transformers. In *2021 IEEE/CVF Conference on Computer Vision and Pattern Recognition (CVPR)*. IEEE, June 2021.
- [16] Y. Liu, C. Matsoukas, F. Strand, H. Azizpour, and K. Smith. Patch-dropout: Economizing vision transformers using patch dropout. *ArXiv*, abs/2208.07220, 2022.
- [17] H. Ma, L. Chen, D. Kong, Z. Wang, X. Liu, H. Tang, X. Yan, Y. Xie, S.-Y. Lin, and X. Xie. Transfusion: Cross-view fusion with transformer for 3d human pose estimation. In *British Machine Vision Conference*, 2021.
- [18] H. Ma, Z. Wang, Y. Chen, D. Kong, L. Chen, X. Liu, X. Yan, H. Tang, and X. Xie. PPT: token-pruned pose transformer for monocular and multi-view human pose estimation. In *European Conference on Computer Vision*, 2022.
- [19] N. Mahmood, N. Ghorbani, N. F. Troje, G. Pons-Moll, and M. J. Black. AMASS: Archive of motion capture as surface shapes. In *International Conference on Computer Vision*, pages 5442–5451, Oct. 2019.
- [20] W. Mao, Y. Ge, C. Shen, Z. Tian, X. Wang, Z. Wang, and A. v. d. Hengel. Poseur: Direct human pose regression with transformers. In *Proceedings of the European Conference on Computer Vision (ECCV)*, October 2022.
- [21] J. Martinez, R. Hossain, J. Romero, and J. J. Little. A simple yet effective baseline for 3d human pose estimation. In *ICCV*, 2017.
- [22] B. Mildenhall, P. P. Srinivasan, M. Tancik, J. T. Barron, R. Ramamoorthi, and R. Ng. NeRF: Representing scenes as neural radiance fields for view synthesis. In *ECCV*, 2020.
- [23] F. Moreno-Noguer. 3d human pose estimation from a single image via distance matrix regression. In *2017 IEEE Conference on Computer Vision and Pattern Recognition (CVPR)*, pages 1561–1570, Los Alamitos, CA, USA, jul 2017. IEEE Computer Society.
- [24] G. Pavlakos, X. Zhou, K. G. Derpanis, and K. Daniilidis. Harvesting multiple views for marker-less 3d human pose annotations. In *Proceedings of the IEEE Conference on Computer Vision and Pattern Recognition (CVPR)*, July 2017.
- [25] D. Pavlo, C. Feichtenhofer, D. Grangier, and M. Auli. 3D human pose estimation in video with temporal convolutions and semi-supervised training. In *2019 IEEE/CVF Conference on Computer Vision and Pattern Recognition (CVPR)*. IEEE, June 2019.
- [26] J. Plücker. *On a New Geometry of Space*. Royal Society, 1865.
- [27] H. Qiu, C. Wang, J. Wang, N. Wang, and W. Zeng. Cross view fusion for 3D human pose estimation. *ICCV 2019*, 2019.
- [28] W. Qiu, F. Zhong, Y. Zhang, S. Qiao, Z. Xiao, T. S. Kim, and Y. Wang. UnrealCV: Virtual worlds for computer vision. In *Proceedings of the 25th ACM international conference on Multimedia*, MM '17, pages 1221–1224, New York, NY, USA, Oct. 2017. Association for Computing Machinery.
- [29] E. Remelli, S. Han, S. Honari, P. Fua, and R. Wang. Lightweight multi-view 3d pose estimation through camera-disentangled representation. In *2020 IEEE/CVF Conference on Computer Vision and Pattern Recognition (CVPR)*, pages 6039–6048, jun 2020.
- [30] H. Rhodin, F. Meyer, J. Spoerri, E. Müller, V. Constantin, I. Katircioglu, P. Fua, and M. Salzmann. Learning monocular 3d human pose estimation from multi-view images. In *IEEE/CVF 2018 Conference on Computer Vision and Pattern Recognition*. IEEE, June 2018.
- [31] I. Sárádi, T. Linder, K. O. Arras, and B. Leibe. How robust is 3D human pose estimation to occlusion? Aug. 2018.
- [32] V. Sitzmann, S. Rezkchikov, W. T. Freeman, J. B. Tenenbaum, and F. Durand. Light field networks: Neural scene representations with Single-Evaluation rendering. In *Proc. NeurIPS*, 2021.
- [33] K. Sun, B. Xiao, D. Liu, and J. Wang. Deep high-resolution representation learning for human pose estimation. In *Proceedings of the IEEE/CVF Conference on Computer Vision and Pattern Recognition*, pages 5693–5703, 2019.
- [34] A. Vaswani, N. Shazeer, N. Parmar, J. Uszkoreit, L. Jones, A. N. Gomez, Ł. U. Kaiser, and I. Polosukhin. Attention is all you need. In I. Guyon, U. V. Luxburg, S. Bengio, H. Wallach, R. Fergus, S. Vishwanathan, and R. Garnett, editors, *Advances in Neural Information Processing Systems*, volume 30. Curran Associates, Inc., 2017.
- [35] N. Venkat, M. Agarwal, M. Singh, and S. Tulsiani. Geometry-biased

transformers for novel view synthesis. Jan. 2023.

- [36] T. Wehrbein, M. Rudolph, B. Rosenhahn, and B. Wandt. Probabilistic monocular 3D human pose estimation with normalizing flows. In *International Conference on Computer Vision (ICCV)*, 2021.
- [37] H. Xia and Q. Zhang. VitPose: Multi-view 3D human pose estimation with vision transformer. In *2022 IEEE 8th International Conference on Computer and Communications (ICCC)*, pages 1922–1927, Dec. 2022.
- [38] R. Xie, C. Wang, and Y. Wang. Metafuse: A pre-trained fusion model for human pose estimation. In *2020 IEEE/CVF Conference on Computer Vision and Pattern Recognition (CVPR)*, pages 13683–13692, Los Alamitos, CA, USA, jun 2020. IEEE Computer Society.
- [39] S. Yang, Z. Quan, M. Nie, and W. Yang. Transpose: Keypoint localization via transformer. In *IEEE/CVF International Conference on Computer Vision (ICCV)*, 2021.
- [40] J. Zhang, Z. Tu, J. Yang, Y. Chen, and J. Yuan. Mixste: Seq2seq mixed spatio-temporal encoder for 3d human pose estimation in video. In *Proceedings of the IEEE/CVF Conference on Computer Vision and Pattern Recognition (CVPR)*, pages 13232–13242, June 2022.
- [41] T. Zhang, B. Huang, and Y. Wang. Object-occluded human shape and pose estimation from a single color image. In *2020 IEEE/CVF Conference on Computer Vision and Pattern Recognition (CVPR)*. IEEE, June 2020.
- [42] Z. Zhang, C. Wang, W. Qiu, W. Qin, and W. Zeng. Adafuse: Adaptive multiview fusion for accurate human pose estimation in the wild. *International Journal of Computer Vision*, 129:703 – 718, 2020.